

Electrochemical Preparation of Vertically aligned, Hollow CdSe Nanotubes and its p-n junction Hybrid with Electrodeposited Cu₂O

Joyashish Debgupta,^a Ramireddy Devarapalli,^{a, b} Shakeelur Rahman,^a Manjusha V. Shelke^{a, b} and Vijayamohanan K. Pillai^{a, b, c*}

^aPhysical & Materials Chemistry Division, Dr. Homi Bhabha Road, Pashan, Pune-411008.

^bAcademy of Scientific and Innovative Research (AcSIR), Anusandhan Bhawan, 2 Rafi Marg, New Delhi-110 001.

^cCentral Electrochemical Research Institute, Karaikudi, Tamil Nadu.

E-mail: *vk.pillai@ncl.res.in*

Supporting Information

Figure S1: Cyclic voltammetry of Cd(OAc)₂ using FTO plate as working electrode

Figure S2: Cyclic voltammetry of Na₂SeO₃ using FTO plate as working electrode

Figure S3: Cyclic voltammetry of Cd(OAc)₂, Na₂SeO₃ using FTO plate as working electrode

Figure S4: UV-Vis absorption plots of ZnO NWs-CdSe at different leaching time

Figure S5: PXRD pattern of CdSe nanotubes and ZnO NWs on FTO

Figure S6: PXRD pattern of electrodeposited Cu₂O on FTO

Figure S7: SEM images of electrodeposited Cu₂O on FTO

Figure S8: I-V of CdSe Nanotube-FTO

Figure S9: I-V of Cu₂O-FTO

Figure S10: UV-Vis of electrodeposited Cu₂O on FTO

Figure S11: UV-Vis and Photoluminescence spectra of CdSe nanotubes

Figure S12: Mott-Schottky plots for CdSe NT and Cu₂O film

Figure S13: Photoconductivity with 540 nm and 700 nm light

Figure S14: EDAX of CdSe NT after removal of ZnO core

Figure S15: Chronoamperograms during electrodeposition of CdSe on FTO and on ZnO NW coated FTO

Figure S16: EDAX of ZnO Nanowires

Figure S17: XPS of ZnO Nanowires

Cyclic voltammetry of $\text{Cd}(\text{OAc})_2$ using FTO plate as working electrode:

Fig. S1 shows the cyclic voltammogram of 10 mM $\text{Cd}(\text{OAc})_2$ solution in presence of NTA using FTO coated glass plates. No distinct peak is observed in the voltammogram within the electrochemical window selected (-1.3 V to 1 V vs Hg/HgO reference electrode). This suggests that cadmium deposition is negligible (which is undesirable) during CdSe electrodeposition which has been carried out at -1.2 V. NTA thus serves as good chelating agent (binding constant ~ 9.5) for Cd^{2+} and thereby shifts the reduction potential of Cd^{2+} to far negative value.

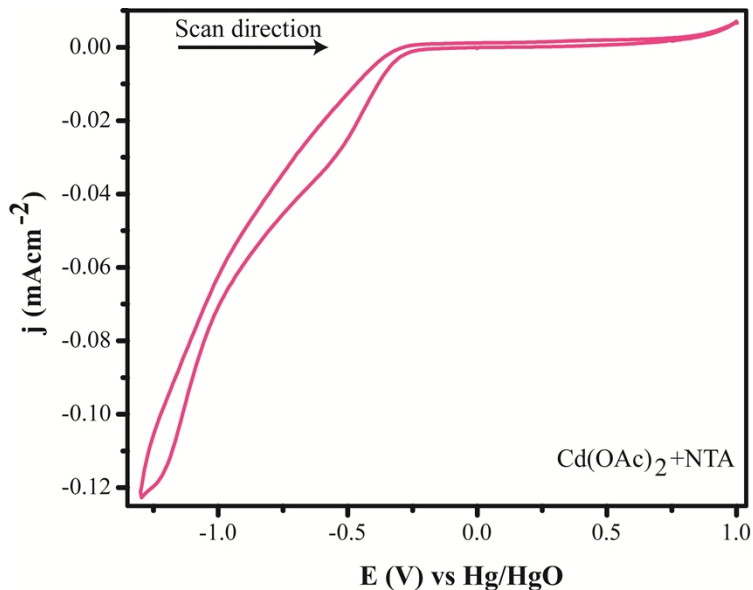


Figure S1. Cyclic voltammetry of $\text{Cd}(\text{OAc})_2$ using FTO plate as working electrode, Pt-foil as CE and Hg/HgO as RE. The solution contains 10 mM $\text{Cd}(\text{OAc})_2$ and 50 mM nitrilotriacetic acid (NTA) and NaOH was added to make the pH 7.5. Scan rate is 20 mV/s.

Cyclic voltammetry of Na_2SeO_3 using FTO plate as working electrode:

Cyclic voltammogram of 5 mM Na_2SeO_3 (Figure S2) shows two distinctive reduction peaks (C1 and C2) using FTO plate as working electrode and in absence of NTA. The two peaks correspond respectively to SeO_3^{2-} to Se and Se to Se^{2-} species. Se^{2-} is the reactive species which forms CdSe on reacting with Cd-NTA complex. There is also one anodic peak (A1) observed in the voltammogram. This peak is probably due to the oxidation of Se^{2-} to Se.

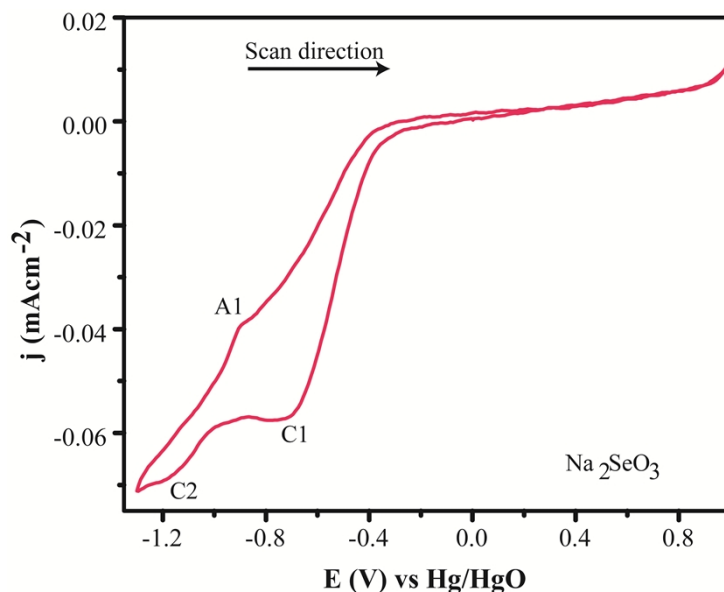


Figure S2. Cyclic voltammetry of Na_2SeO_3 using FTO plate as working electrode, Pt-foil as CE and Hg/HgO as RE. The solution contains 5 mM Na_2SeO_3 . Scan rate is 20 mV/s.

Cyclic voltammetry of $\text{Cd}(\text{OAc})_2$, Na_2SeO_3 using FTO plate as working electrode:

Voltammogram of a mixture of $\text{Cd}(\text{OAc})_2$ and Na_2SeO_3 in presence of NTA (FTO plate as working electrode) also shows two distinctive cathodic peaks C1 and C2 but no anodic peak is observed. Since C1 and C2 are observed only in presence of SeO_3^{2-} , the peaks carry the same significance as for only Na_2SeO_3 . Moreover, disappearance of anodic peak (A1) unlike that in case of SeO_3^{2-} alone, indicates the formation of CdSe involving reaction between Cd-NTA and Se^{2-} . Thus the proposed mechanism of electrodeposition of CdSe can be unraveled.

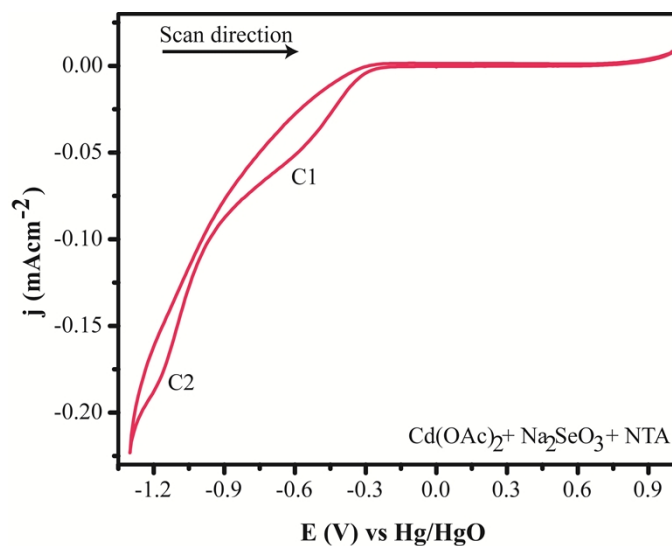


Figure S3. Cyclic voltammetry of Na_2SeO_3 using FTO plate as working electrode, Pt-foil as CE and Hg/HgO as RE. The solution contains 10 mM $\text{Cd}(\text{OAc})_2$, 5 mM Na_2SeO_3 and 50 mM nitrilotriacetic acid (NTA) and NaOH was added to make the pH 7.5. Scan rate is 20 mV/s.

UV-Vis absorption plots of ZnO NWs-CdSe at different leaching time:

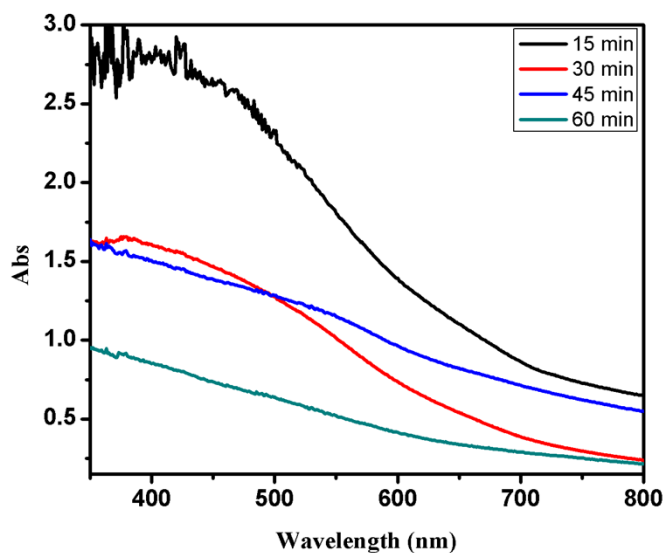


Figure S4. UV-Vis absorption spectra of ZnO NWs-CdSe at different time of leaching ZnO NWs with 25% NH_4OH solution. The plateau within the range 550-350 nm corresponds to ZnO absorption and is found to decrease with increase in leaching time. This indicates gradual removal of ZnO and forming CdSe nanotubes.

PXRD pattern of CdSe nanotubes and ZnO NWs on FTO:

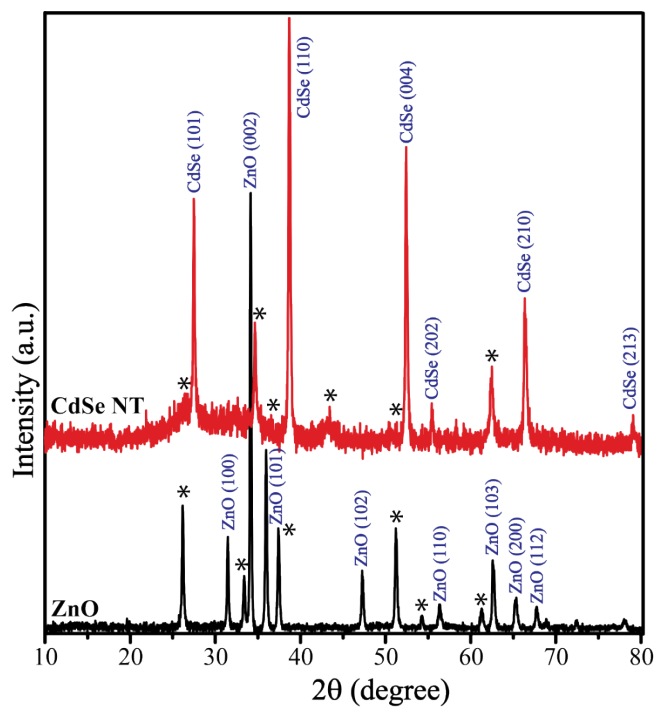


Figure S5. Powder X-ray diffraction pattern of ZnO nanowires and CdSe nanotubes grown on FTO coated glass plates. No ZnO diffraction is observed after removal of ZnO core. (*) indicates peaks from FTO coated glass substrate.

PXRD pattern of electrodeposited Cu_2O on FTO:

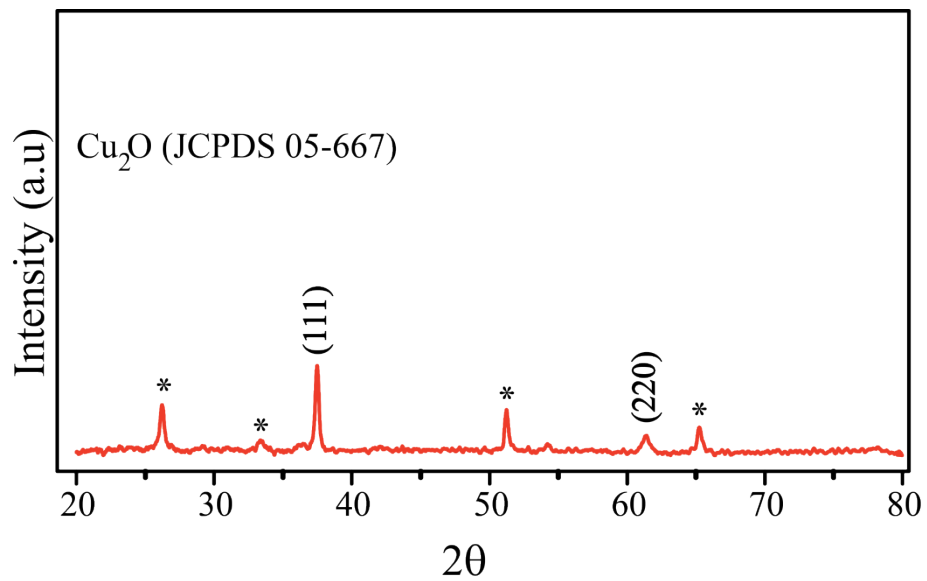


Figure S6. Powder X-ray diffraction pattern of Cu_2O film electrodeposited on FTO coated glass plates. (*) indicates peaks from FTO coated glass substrate. The reflections match well with JCPDS 05-667 reflections.

SEM images of electrodeposited Cu_2O on FTO:

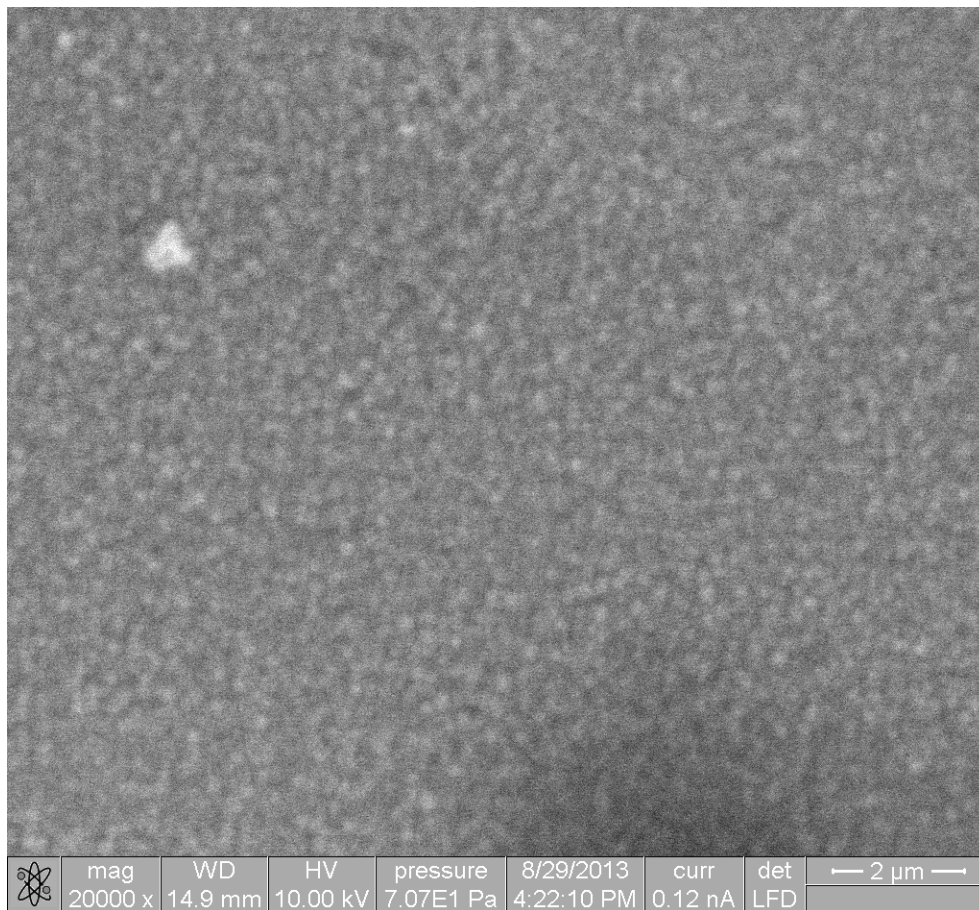


Figure S7. Scanning electron micrograph of electrodeposited Cu_2O film on FTO coated glass plate. Uniform coating is observed throughout the substrate.

I-V of CdSe Nanotube-FTO:

CdSe nanotubes (CdSe NT) show Schottky type symmetric plot with respect to forward and reverse biases.

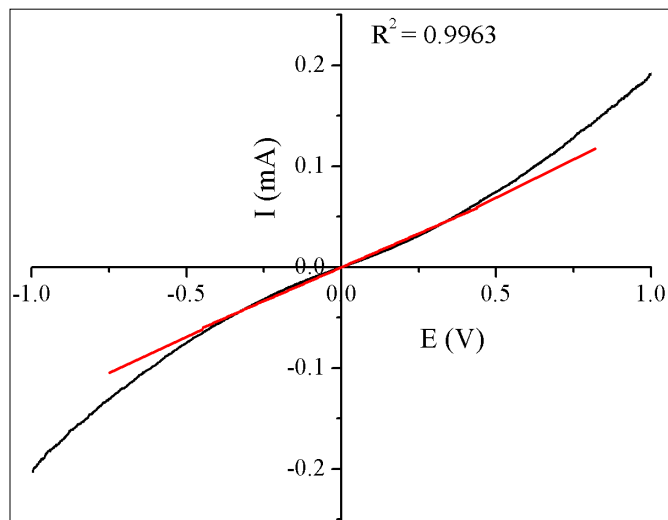


Figure S8. Current-voltage (I-V) characteristic of CdSe nanotube/FTO junction; red line shows the linear fit of the plot for ohmic behavior. CdSe nanotube film is flip-chipped with FTO coated glass plate.

I-V of Cu₂O film-FTO:

Electrodeposited Cu₂O film shows Schottky type behavior with respect to forward and reverse biases. For Ohmic and Schottky junctions, the current (I) is related to voltage (V) as follows:[1]

$$I = \frac{E}{R} \dots\dots\dots(1) \text{ (Ohmic)}$$

Where, I = current, E = voltage and R = resistance

$$I = I_0 \exp\left[\frac{e}{kT} \left(\frac{eE}{4\pi\epsilon_0}\right)^{\frac{1}{2}}\right] \dots\dots\dots(2) \text{ (Schottky)}$$

Equation 2 can be rewritten as,

$$\ln I = \ln I_0 + K.E^{\frac{1}{2}} \dots\dots\dots(3)$$

Where, $K = \left[\frac{e}{kT} \left(\frac{e}{4\pi\epsilon_0}\right)^{\frac{1}{2}} \right] = \text{constant}$

e = electronic charge, k = Boltzmann constant, T = absolute temperature and ε₀= permittivity of vacuum.

According to equation 1, plot of I vs V should produce a straight line passing through zero. On the other hand, plot of lnI vs E^{1/2} should give a straight line with an intercept lnI₀ on the ordinate (i.e., lnI axis). Fig. S9 (c) shows that at very low voltage range (± 0.04 V), current follows a linear relationship with applied voltage, i.e., ohmic behavior predominates. But at voltages larger than this threshold value, the observed current follows Schottky type behavior as is seen from fig. S9 (b). The plot (fig. S9 (b)) shows nonlinear behavior below 0.04 V indicating deviation from Schottky type below this threshold voltage. Thus Cu₂O/FTO junction shows mixed type behavior.

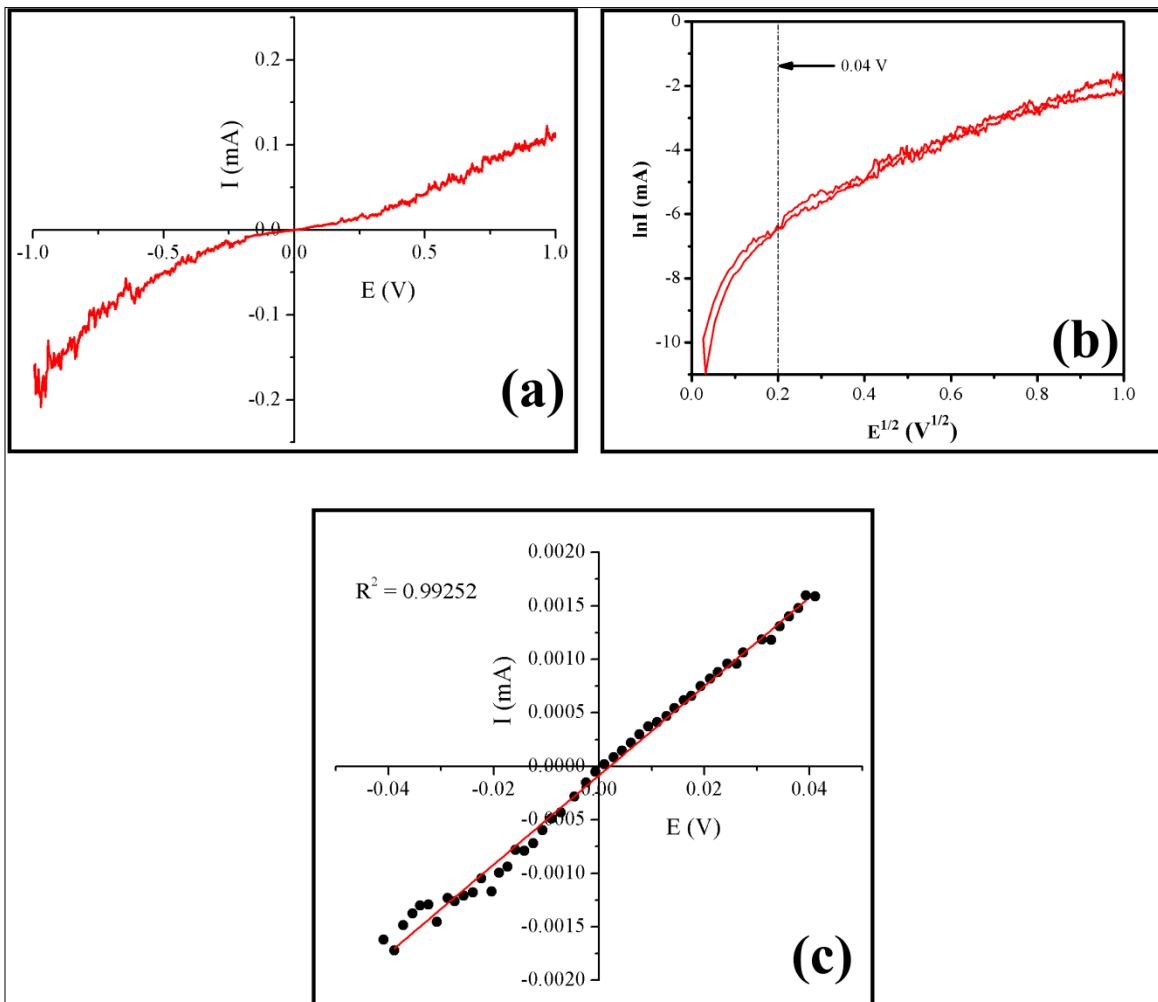


Figure S9. (a) Current-voltage characteristic of Cu₂O/FTO junction; (b) ln I vs E^{1/2} plot for testing Schottky behavior; (c) linear fit of the I-V curve at very low voltage (within ± 0.04 V). Cu₂O film is flip-chipped with FTO coated glass plate.

UV-Vis spectra of electrodeposited Cu₂O on FTO:

Figure S10 shows the UV-Vis spectrum of electrodeposited thin film of Cu₂O in solid state. The absorption spectrum clearly shows one broad hump at 650 nm, corresponding to CuO formed during the exposure of the Cu₂O sample in the atmosphere, and two peaks with λ_{\max} 452 nm and 340 nm. The peak at 452 nm corresponds to the band edge transition for p-type Cu₂O and the other peak at 340 nm is due to band-to-band transition in Cu₂O.^[2]

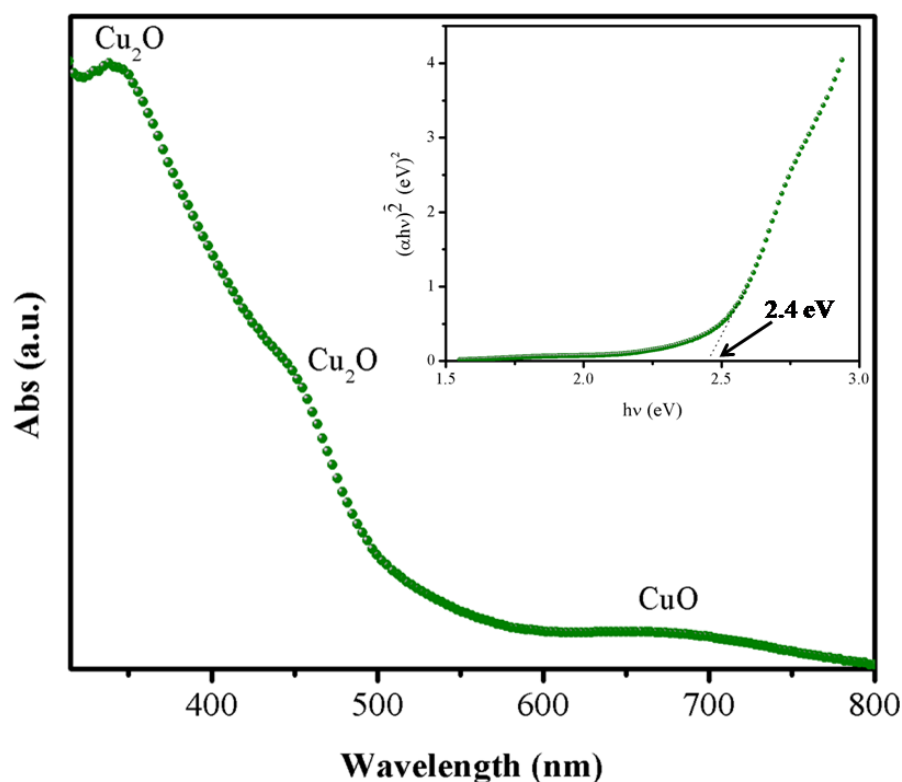


Figure S10. UV-Vis absorption spectrum of p-type Cu₂O electrodeposited on FTO coated glass plate. Inset shows the corresponding Tauc plot showing the direct band gap transition for the material (Cu₂O).

UV-VIS and Photoluminescence spectra of CdSe nanotubes:

UV-VIS absorbance and photoluminescence (PL) spectra of CdSe nanotubes are displayed in Fig. S11 (a) and (b). The onset of absorption for CdSe NTs is 750 nm (Figure S11 (a)), which corresponds to ~ 1.7 eV, i.e., the optical band-gap value of bulk CdSe.^[3] This is expected because the CdSe NPs (8-10 nm) which form the CdSe NTs are far from the strong quantum confinement region (exciton Bohr radius is 5.4 nm). The maximum absorption occurs at 650 nm and is related to the first excitonic transition (1s-1p) in CdSe.^[4] In comparison, CdSe NTs show a broad emission spectrum centered around 662 nm in the PL (Figure 7(b)) with a Stokes shift of ~ 13 nm (37.6 meV). This is in accordance with the reported literature.^[5]

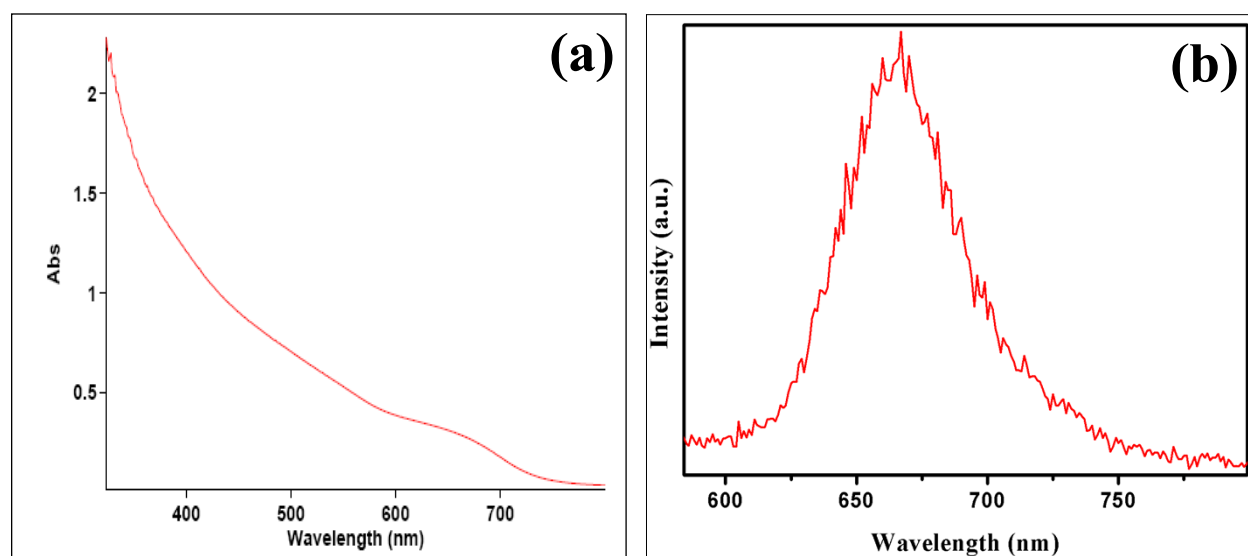


Figure S11. (a) UV-Visible absorbance and (b) corresponding photoluminescence (PL) spectra of CdSe nanotubes. PL spectrum is recorded after exciting the nanotubes at 650 nm which is the excitonic maximum of CdSe NTs in absorbance spectrum.

Mott-Schottky plots for CdSe NT and Cu₂O film:

Capacitance measurement on the electrode/electrolyte interface has been carried out to determine the flat band (E_{fb}) potential of the material and carrier density (N_A), which are important parameters to describe a semiconductor electrode/electrolyte interface. When a semiconductor comes in contact with an electrolyte solution, semiconductor Fermi level tends to align itself with the Fermi level of the electrolyte solution, until equilibrium is established. As a result, the valence and conduction bands shift upward or downward (depending on the position of the two Fermi levels before contact). E_{fb} is a measure of the extent of band bending when a semiconductor electrode is brought in contact with an electrolyte solution. Both E_{fb} and carrier density (N_A) can be determined from Mott-Schottky plot which is a plot of $1/C^2$ vs applied potential at a fixed frequency (where, C is the space charge capacitance of the semiconductor) of 20 kHz. The capacitance measurements are presented as an MS plot following the equation below (Mott-Schottky equation):^[6]

$$\frac{1}{C^2} = \frac{2}{N_A \epsilon \epsilon_0 e} \left[E - E_{fb} - \frac{kT}{e} \right] \dots\dots\dots(6)$$

Where, C is the interfacial capacitance (i.e., capacitance of the semiconductor depletion layer), ϵ is the dielectric constant of the material, ϵ_0 is the permittivity of free space ($8.85 \times 10^{-12} \text{ Fm}^{-1}$), N_A is the number density (cm^{-3}) of donors/acceptors in the semiconductor (doping level), E is the applied potential, E_{fb} is the flat band potential, T is the absolute temperature (298 K), k is the Boltzmann constant ($1.38 \times 10^{-23} \text{ JK}^{-1}$) and e is the electron charge ($1.6 \times 10^{-19} \text{ C}$). The temperature term is generally small and can be neglected. Fig. 5.13 shows Mott-Schottky (MS) plot for both CdSe NTs and Cu₂O. Nature of the plots suggests that CdSe is an n-type and Cu₂O

is a p-type semiconductor. Moreover, the intercept of the plot on potential (E) axis (at $y = 0$) is the E_{fb} of the material for a specific electrode /electrolyte interface. Hence, the E_{fb} of CdSe NTs is $-0.76 \text{ V vs Hg/HgO}$ and that for Cu_2O is 0.92 V vs Hg/HgO at room temperature (303 K). Carrier density (N_A) as calculated from the slope of the MS plot is found to be $7.3 \times 10^{16} \text{ m}^{-3}$ for CdSe NTs (electron is the majority carrier) and $1.09 \times 10^{17} \text{ m}^{-3}$ for Cu_2O (hole is the majority carrier).

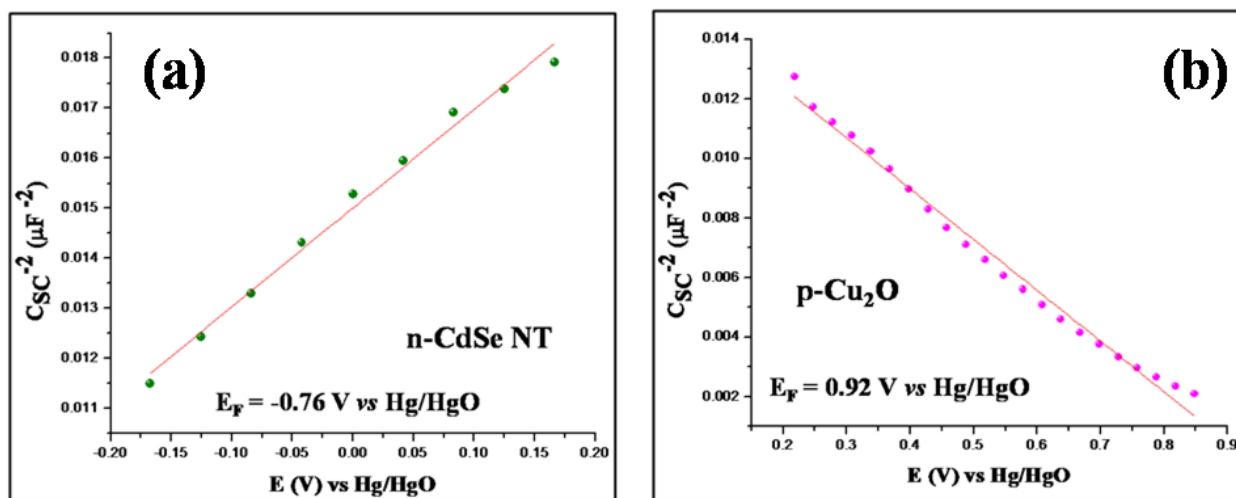


Figure S12. Mott-Schottky plot for (a) n-type CdSe NTs and (b) p-type Cu_2O . Impedance is carried out in $\text{Na}_2\text{S-Na}_2\text{SO}_3$ solution for CdSe NTs and in 0.1 M NaOAc aq. solution for Cu_2O . Nature of the plots suggests that CdSe NT is n-type semiconductor and electrodeposited Cu_2O is p-type semiconductor. Solutions and potential ranges are chosen in such a way that the chemical composition of the materials do not change during the measurement.

Photoconductivity with 540 nm and 700 nm light:

Photoconductivity of the device has been tested by illuminating 540 nm and 700 nm monochromatic light from Cu₂O side. The device shows larger photoresponse at 700 nm as compared to that at 540 nm because of larger inner as well as outer surface area of CdSe nanotubes which absorbs much of the incident light and generates large numbers of exciton per unit area.

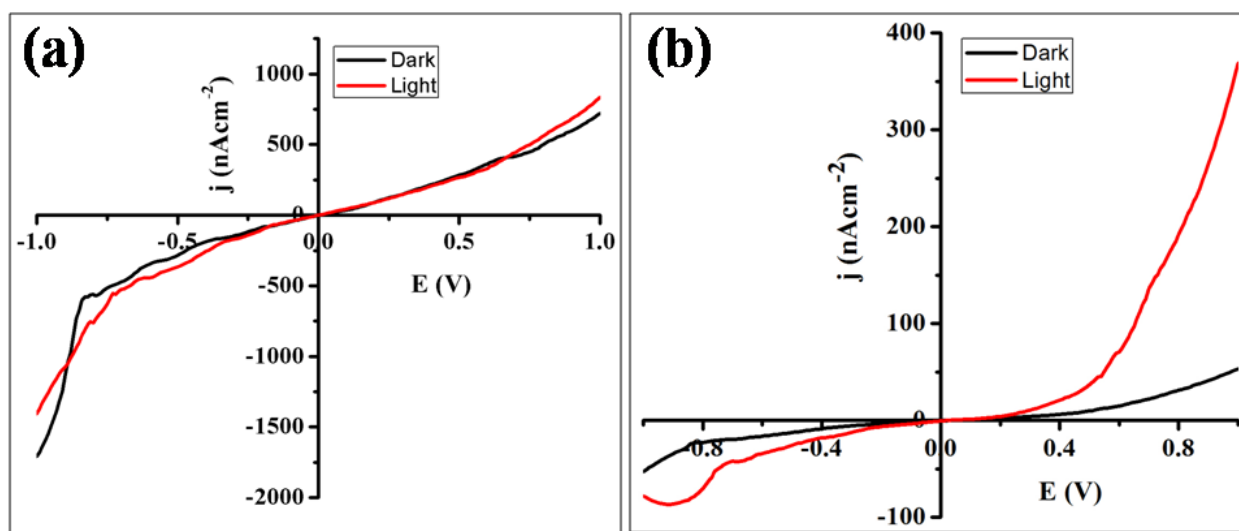


Figure S13. Photoconductivity of the n-p heterojunction device with (a) 540 nm and (b) 700 nm illumination respectively; higher photocurrent is observed with 700 nm illumination.

EDAX of CdSe NT after removal of ZnO core:

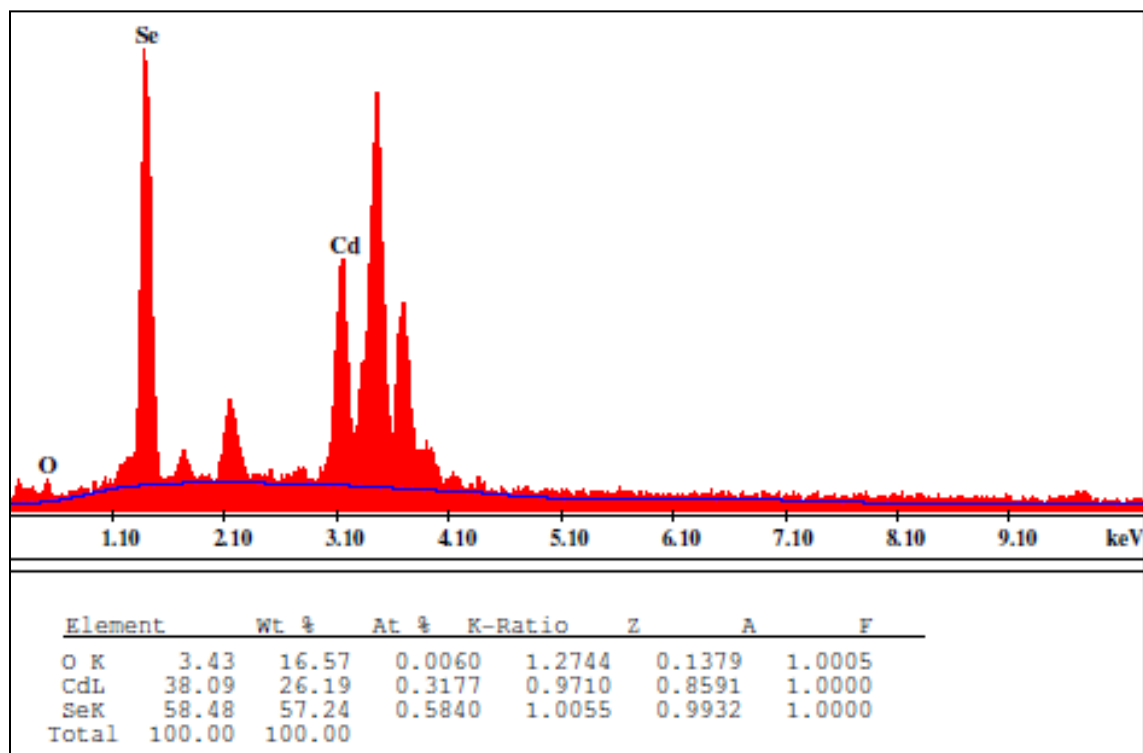


Figure S14. Elemental analysis (EDAX) of CdSe electrodeposited on FTO coated glass plates using ZnO NW template. No ZnO peak is detected because of leaching out of the same by NH_4OH leading to nanotubes.

Chronoamperograms during electrodeposition of CdSe on FTO and on ZnO NW coated

FTO:

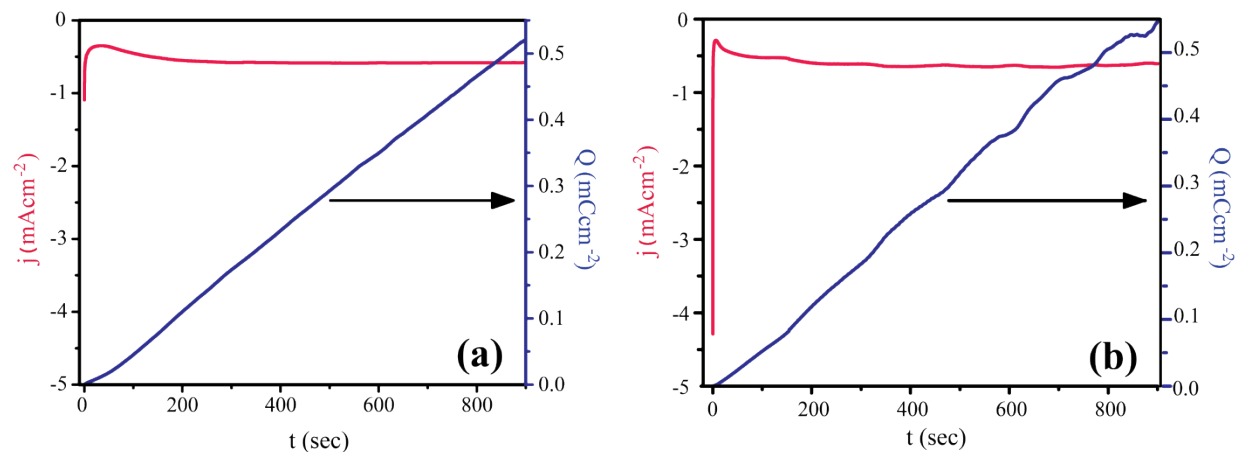


Figure S15. Chronoamperograms (pink line) during CdSe electrodeposition on (a) plain FTO coated glass plate and (b) ZnO NW coated glass plate. Blue line indicates total charge passed during electrodeposition. Chronoamperometry experiments are carried out with the same set up used for cyclic voltammetry and the potential of the working electrode (FTO or ZnO NW coated FTO) are held constant at -1.2 V vs Hg/HgO electrode for 15 min. Temperature is kept constant at room temperature (303 K). Total charge passed is same in both the cases.

EDAX analysis of ZnO Nanowires:

A single ZnO NW has been scanned in TEM in order to understand the surface composition of the NW. Accordingly, fig. S16 shows the EDAX plot of the ZnO NW. This clearly shows that the surface as well as bulk of the ZnO NW is composed of only zinc (Zn) and oxygen (O) and thereby rules out the possibility of any surface contaminant (such as any surfactant).

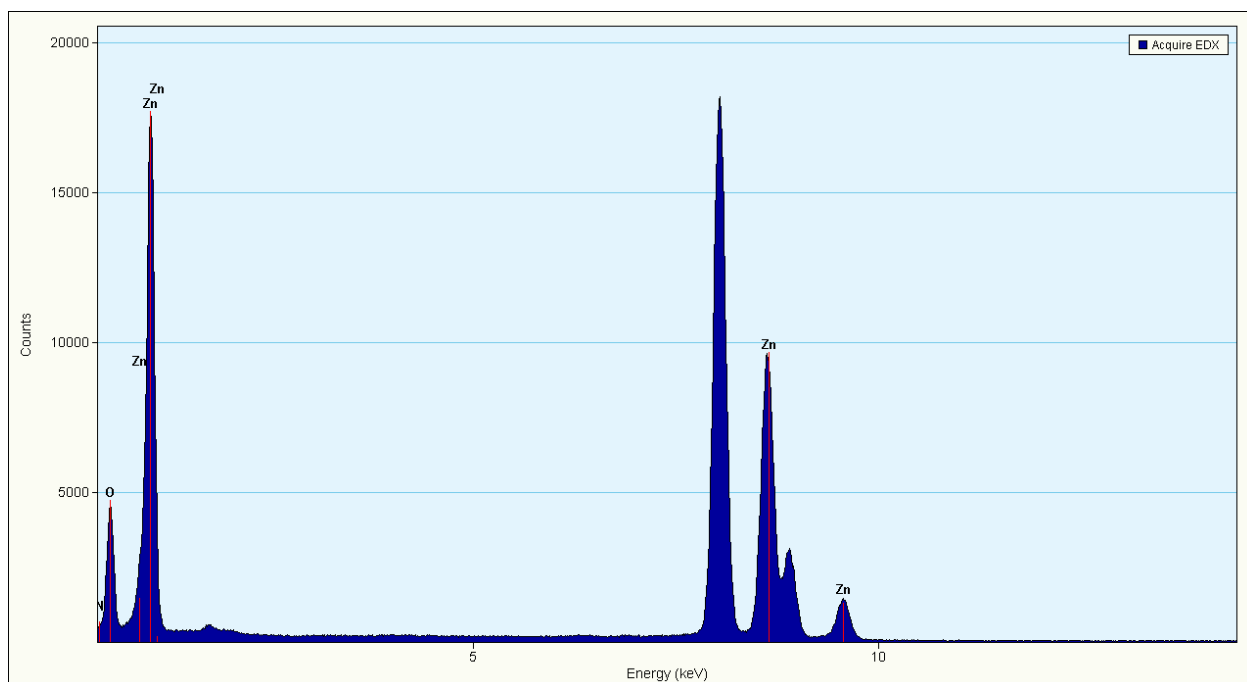


Figure S16. Elemental analysis (EDX) of pure ZnO NWs vertically grown on FTO coated glass plates; a single nanowire has been scanned for better understanding the surface composition.

XPS Analysis of ZnO Nanowires:

XPS was recorded in a custom-built laboratory based ambient pressure photoelectron spectrometer in UHV mode (base pressure 1×10^{-10} mbar). It is equipped with Al-K alpha monochromator (MX650 VG Scienta), Al K alpha-Mg K alpha twin anode (XR40B Prevac) X-ray sources and R3000 HP VG Scienta analyzer.⁶

Fig. S17 shows the survey scan of ZnO NWs vertically grown on FTO coated glass plate. Peaks for only Zn^{2+} and O^{2-} are only visible in the spectrum along with small peaks for SiO_2 which comes from glass.⁶ Absence of any other peaks clearly indicates the absence of any surface contamination on the as grown ZnO NWs.

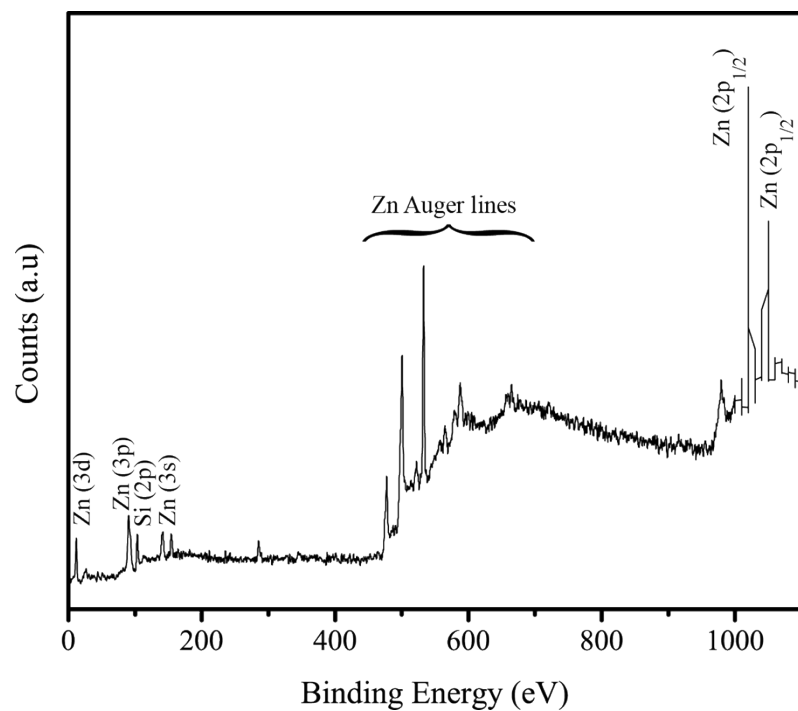


Figure S17. Survey scan XPS spectrum of ZnO NWs grown directly on FTO coated glass plate; Al K-alpha lines are used for recording the spectrum.

References:

- [1] S. M. Sze and K. K. Ng, *Physics of semiconductor devices*. John Wiley & Sons., 2006
- [2] M. Yin, C. K. Wu, Y. Lou, C. Burda, J. T. Koberstein, Y. Zhu, S. O'Brien, *J. Am. Chem. Soc.* 2005, 127(26), 9506.
- [2] R. B. Parson, W. Wardzynski, A. D. Yoffe, R. B. Parsons, *Pro. Royal Soc. London. Series A. Mathematical and Physical Sciences* 1961, 2628, 120.
- [3] M. C. Troparevsky, L. Kronik, J. R. Chelikowsky, *J. Chem.. Phys.* 2003, 119, 2284.
- [4] M. Zhou, H. Zhu, X. Wang, Y. Xu, Y. Tao, S. Hark, Q. Li, *Chem. Mater.* 2009, 22, 64.

- [5] A. J. Bard and L. R. Faulkner, *Electrochemical methods: fundamentals and applications*, Vol. 2. New York: Wiley, 1980.
- [6] (a) K. Roy, C. P. Vinod, C. S. Gopinath, *J. Phys. Chem. C*, **2013**, 117 (9), 4717. (b) K. Roy, C. S. Gopinath, *Anal. Chem.* **2014**, 86 (8), 3683. (c) M. Mapa, C. S. Gopinath, *Chem. Mater.* **2008**, 21(2), 351.